

# PROOF COVER SHEET

---

Author(s): T. Rétornaz, J.-M. Friedt, S. Alzuaga, T. Baron, É. Lebrasseur, G. Martin, T. Laroche, S. Ballandras, M. Griselin, J.-P. Simonnet

Article title: Piezoelectric radiofrequency transducers as passive buried sensors

Article no: 674524

Enclosures: 1) Query sheet  
2) Article proofs

---

Dear Author,

**1. Please check these proofs carefully.** It is the responsibility of the corresponding author to check these and approve or amend them. A second proof is not normally provided. Taylor & Francis cannot be held responsible for uncorrected errors, even if introduced during the production process. Once your corrections have been added to the article, it will be considered ready for publication.

Please limit changes at this stage to the correction of errors. You should not make insignificant changes, improve prose style, add new material, or delete existing material at this stage. Making a large number of small, non-essential corrections can lead to errors being introduced. We therefore reserve the right not to make such corrections.

For detailed guidance on how to check your proofs, please see <http://journalauthors.tandf.co.uk/production/checkingproofs.asp>.

---

**2. Please review the table of contributors below and confirm that the first and last names are structured correctly and that the authors are listed in the correct order of contribution.** This check is to ensure that your name will appear correctly online and when the article is indexed.

Sequence	Prefix	Given name(s)	Surname	Suffix
1.		T.	Rétornaz	
2.		J.-M.	Friedt	
3.		S.	Alzuaga	
4.		T.	Baron	
5.		É.	Lebrasseur	
6.		G.	Martin	

7.		T.	Laroche	
8.		S.	Ballandras	
9.		M.	Griselin	
10.		J.-P.	Simonnet	

Queries are marked in the margins of the proofs.

## AUTHOR QUERIES

General query: You have warranted that you have secured the necessary written permission from the appropriate copyright owner for the reproduction of any text, illustration, or other material in your article. (Please see <http://journalauthors.tandf.co.uk/preparation/permission.asp>.) Please check that any required acknowledgements have been included to reflect this.

- AQ1** Please check the sense of the sentence.
- AQ2** Please provide location details for references [1,5,6,10,17–19,22,24–27,31,34,35].
- AQ3** Please check the inserted publisher location details for reference [3].
- AQ4** Please provide volume details for reference [7].
- AQ5** Please check the details in reference [25].

## How to make corrections to your proofs using Adobe Acrobat

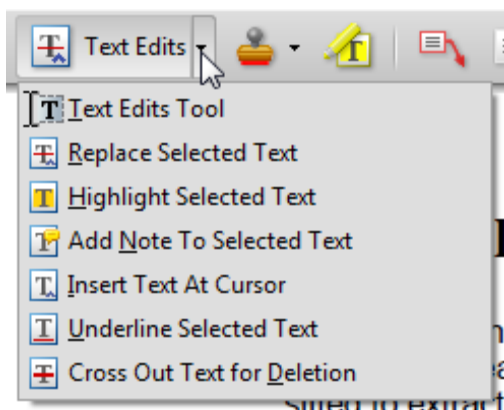
Taylor & Francis now offer you a choice of options to help you make corrections to your proofs. Your PDF proof file has been enabled so that you can edit the proof directly using Adobe Acrobat. This is the simplest and best way for you to ensure that your corrections will be incorporated. If you wish to do this, please follow these instructions:

1. Save the file to your hard disk.
2. Check which version of Adobe Acrobat you have on your computer. You can do this by clicking on the “Help” tab, and then “About.”

If Adobe Reader is not installed, you can get the latest version free from <http://get.adobe.com/reader/>.

- If you have Adobe Reader 8 (or a later version), go to “Tools”/ “Comments & Markup”/ “Show Comments & Markup.”
- If you have Acrobat Professional 7, go to “Tools”/ “Commenting”/ “Show Commenting Toolbar.”

3. Click “Text Edits.” You can then select any text and delete it, replace it, or insert new text as you need to. If you need to include new sections of text, it is also possible to add a comment to the proofs. To do this, use the Sticky Note tool in the task bar. Please also see our FAQs here: <http://journalauthors.tandf.co.uk/production/index.asp>.



4. Make sure that you save the file when you close the document before uploading it to CATS using the “Upload File” button on the online correction form. A full list of the comments and edits you have made can be viewed by clicking on the “Comments” tab in the bottom left-hand corner of the PDF.

If you prefer, you can make your corrections using the CATS online correction form.



## Piezoelectric radiofrequency transducers as passive buried sensors

T. Rétoznaz<sup>a</sup>, J.-M. Friedt<sup>a\*</sup>, S. Alzuaga<sup>b</sup>, T. Baron<sup>b</sup>, É. Lebrasseur<sup>b</sup>, G. Martin<sup>b</sup>,  
T. Laroche<sup>b</sup>, S. Ballandras<sup>a,b</sup>, M. Griselin<sup>c</sup> and J.-P. Simonnet<sup>d</sup>

<sup>a</sup>*SENSeOR SAS, Besançon, France;* <sup>b</sup>*Time & Frequency Department, Institut FEMTO-ST, UMR  
CNRS 6174, Besançon, France;* <sup>c</sup>*Laboratoire ThéMA, UMR CNRS 6049, Besançon, France;*  
<sup>d</sup>*Laboratoire Chrono-Environnement, UMR CNRS 6249, Besançon, France*

(Received 9 October 2011; final version received 23 February 2012)

We demonstrate that single-piezoelectric substrate-based acoustic transducers act as ideal sensors for probing with various RADAR strategies. Because these sensors are intrinsically passive devices working in the radiofrequency range, they exhibit improved interrogation range and robustness with respect to silicon-based radiofrequency identification tags. Both wideband (acoustic delay lines) and narrowband (acoustic resonators) *transducers* are shown to be compatible with pulse-mode and frequency-modulated continuous-wave RADAR strategies, respectively. We particularly focus on the ground-penetrating RADAR (GPR) application in which the lack of local energy source makes these sensors suitable candidates for buried applications in roads, building or civil engineering monitoring. A novel acoustic sensor concept – high-overtone bulk acoustic resonator – is especially suited as sensor interrogated by a wide range of antenna set, as demonstrated with GPR units working in the 100 and 200 MHz range.

**Keywords:** ground-penetrating RADAR; acoustic wave sensor; piezoelectric substrate; wireless interrogation; passive sensor; HBAR

### 1. Introduction

Ground-penetrating RADAR (GPR) is a classical tool for nondestructive observation of buried structures and interfaces, both for geophysical purposes or civil engineering [1] and road-ageing assessment [2–4]. More generally, various RADAR strategies are used for monitoring liquid and granular media level [5,6] or target velocities. In such uses, the measurement is limited to electromagnetic wave reflection by dielectric permittivity or conductivity interfaces.

We aim here to demonstrate how acoustic wave sensors provide an ideal match to classical RADAR measurement techniques in order to provide passive sensors interrogated through a wireless link [7,8]. Surface acoustic wave (SAW) [9] sensors have been demonstrated as transducers for temperature [10–15], stress [16], torque [17], pressure [18–20] and chemisorption monitoring [21–23], as well as for tagging (identification only) applications [24–26]. However, since such devices will only work in a given restricted frequency range compatible with a given RADAR geometry, we extend the demonstration from SAW to a novel bulk acoustic wave resonator configuration operating in a wide frequency range and hence compatible with multiple RADAR antenna geometries. We specifically focus on the

---

\*Corresponding author. Email: jmfriedt@femto-st.fr

50 application of buried sensors interrogated by GPR – with an experimental demonstration  
51 using a pulse mode RADAR and discussion of the frequency-modulated continuous-wave  
52 (FMCW) and frequency-step continuous-wave (FSCW) configurations.

53 The next section will briefly describe RADAR basics and focus on GPR. Section 3 will  
54 summarise the main characteristics of acoustic transducers, while the following sections  
55 will aim at demonstrating the use of both kinds of RADARs targeted to probing the  
56 response of delay lines (Section 3), resonators (Section 4) and the novel high-overtone  
57 bulk acoustic resonator (HBAR) transducer (Section 6).

## 58 59 2. GPR basic principle

60 Classical GPR instrumentation is characterised by two main operation modes: the  
61 wideband pulse-mode GPR and narrowband FMCW and FSCW.

62 Pulse-mode GPR generates a short – wideband – energetic pulse and requires fast  
63 sampling *of the returned signal*: either using an equivalent time sampling [27] strategy for  
64 low-cost operation under the assumption of constant environmental conditions during  
65 the interrogation period (typically several tens of milliseconds), or baseband sampling  
66 thanks to recent fast A/D converters following the software-defined radio approach. The  
67 pulse width is defined by the antenna impedance, which is itself related to the antenna  
68 dimensions and dielectric properties of the surrounding medium. Hence, pulse-mode  
69 GPR will not generate a pulse centred on a known frequency but *operates* at a given  
70 wavelength defined by the dimensions of the emitting antenna. In such a configuration, for  
71 frequencies below 3 GHz, a capacitor is loaded with a high voltage and transfers radiated  
72 energy as a brief pulse thanks to an avalanche transistor whose current versus voltage  
73 characteristics is defined by a positive feedback loop. For a low enough intrinsic  
74 capacitance, the characteristic time needed to empty the high-voltage capacitor as radiated  
75 energy is defined by the resonance frequency of the antenna. Thus, the time constant can  
76 widely vary whether the antenna is surrounded by *low-permittivity* media (ice) or a high-  
77 permittivity environment (liquid water or water-saturated sand for example). This condition  
78 will become a significant hindrance when using a pulse-mode GPR to probe narrowband  
79 resonators which might become out of band when the GPR is used over unsuitable media.

80 In an FMCW – or the related FSCW – a continuous radiofrequency wave is emitted  
81 from one antenna. Either a low-frequency signal is recovered at a beat frequency  
82 proportional to the distance of the reflector (FMCW), or both phase and magnitude of the  
83 returned signals are recovered through I/Q demodulation in the case of an FSCW. Both  
84 strategies provide the needed information to either recover time-domain information  
85 representative of the stratigraphy of the environment through an inverse Fourier transform  
86 under the basic assumption of a constant permittivity of the media through which the  
87 electromagnetic waves propagate, or through more complex analysis of dispersive media  
88 *if both permittivity and reflector depth are identified* [28].

89 Considering that the dielectric properties of the homogeneous materials on both sides  
90 of an interface are known, the reflection coefficient of the electromagnetic wave is *known*  
91 from Fresnel equation under the far-field assumption (plane wave reaching the interface):  
92 this reflection coefficient will be compared with the reflection coefficient of the sensor we  
93 wish to probe using a GPR (Figure 1).

## 94 95 3. SAW delay line basic principle and interrogation strategies

96 SAW transducers are based on the conversion of an incoming electromagnetic wave to a  
97 mechanical wave (inverse piezoelectric effect) propagating at the air–substrate interface,  
98

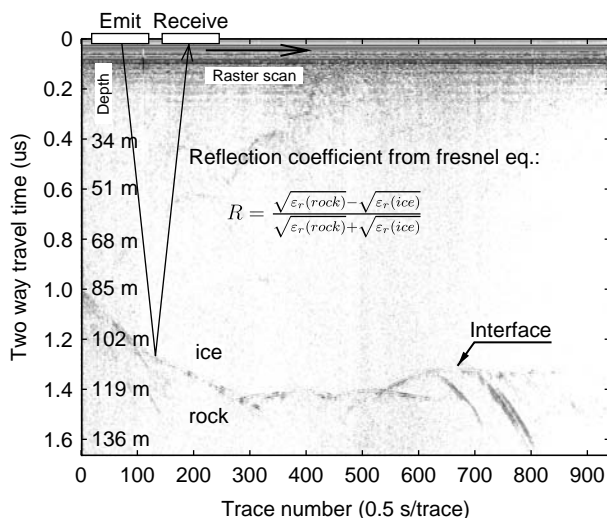


Figure 1. Radargram of a glacier acquired using 100 MHz dipole antennae. The reflection coefficient of an electromagnetic wave generated in a bistatic configuration, reaching in this example the ice-rock interface, is given by the Fresnel equation in the far-field approximation. In a low conductivity medium such as dry ice, the interrogation range is defined by free-space propagation loss and reflection coefficient at the interface. Data recorded at Austre Lovénbreen, Svalbard, Norway.

and then converted back as an electromagnetic wave (direct piezoelectric effect) returned to the reception antenna [29]. As such, the SAW transducer appears as a two-port electrical component, but understanding the underlying measurement principle is mandatory for proper design of the SAW in a sensing application. Since physical conditions of the environment of the transducer induce a change in the acoustic velocity of the mechanical wave propagating on the single-crystal piezoelectric substrate, the reflective radio-frequency properties of the electric dipole ( $S_{11}$  measurement) are indicators of these physical conditions. Under appropriate design conditions, one physical quantity will yield a dominant response with respect to other effects. In order to either perform multiple measurements or decorrelate the contribution of each physical quantity – including the distance of the RADAR antenna to the sensor – a differential approach is used.

The most common SAW sensor configuration is the SAW tag, a wideband device excited by a short electromagnetic pulse and whose returned information is a series of pulses: the number of returned pulses is defined by the number of mirrors patterned through cleanroom lithography techniques on the piezoelectric substrate. For sensing application, only a few mirrors are needed (at least two, one for the reference pulse and the other for the measurement). Coding has been demonstrated with a large number of bits, with over 20 mirrors patterned on the substrate [26]. Since the reflected pulse time interval only provides a rough estimate of the physical quantity due to the minute velocity changes associated with the transducer environment property change, a phase subtraction between successive pulses is classically used to provide a precise measurement of the acoustic velocity and hence physical quantity (Figure 2) [30]. Such a measurement requires either both the returned magnitude and phase information or, as provided by GPR, a baseband measurement of the returned power. Since baseband sampling at several times the central frequency – sampling at 500–40000 MHz for central frequencies typically in the 50–1500 MHz range – is technically challenging and hardly compatible with embedded, low power designs [31], an equivalent time sampling assuming a slowly varying environment

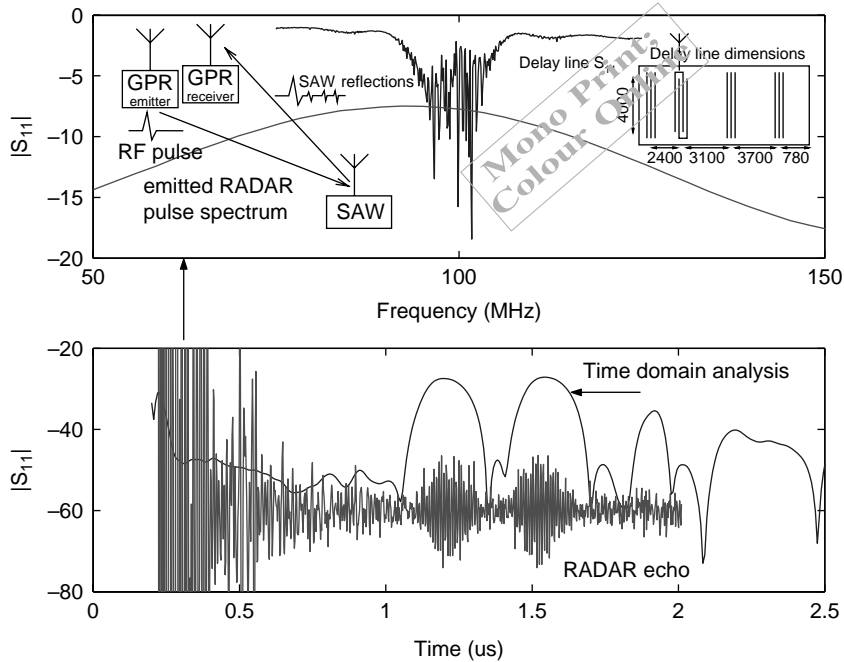


Figure 2. Top: experimental frequency domain characterisation of the 100-MHz Malå RAMAC GPR pulse (red) and transfer function of a SAW delay line (blue) – schematic of the delay line with all dimensions in  $\mu\text{m}$ . Bottom: time-domain signal returned by the SAW when probed using a GPR (red) and network analyser characterisation by inverse Fourier transform of the frequency-domain characterisation (blue).

of the reflectors is often used. In such a strategy,  $N$  successive measurements are carried out at times  $N \times \Delta\tau$  after the excitation pulse is emitted, yielding a series of  $N$  samples separated by a time interval  $\Delta\tau$  or an equivalent sampling rate of  $1/\Delta\tau$ . Hence, the challenge of sampling at 40 G samples/s is replaced with a slow analogue-to-digital converter measuring the voltage recorded by a fast sample-and-hold with 25 ps accuracy (7.5 mm-long transmission line in vacuum). Typical time-domain reflections are in the range of 1–5  $\mu\text{s}$  since the acoustic velocity is typically in the range of 3000–5000 m/s depending on the piezoelectric substrate and the kind of acoustic wave propagating, yielding sensors with dimensions in the centimetre range (a 5  $\mu\text{s}$  delay at 5000 m/s requires a 1.25 mm long acoustic path). Five microseconds are a typical measurement interval for GPR associated with a 425 m deep interface in ice for example (the electromagnetic velocity in ice is assumed to be 170 m/ $\mu\text{s}$  in this example [32]), beyond the typical attenuation range of the electromagnetic pulse.

In an alternative configuration, the acoustic wave is confined between two Bragg mirrors, providing energy confinement conditions consistent with a narrowband transfer function, or in terms of time-domain analysis a long energy dissipation time. In such a configuration, the usable returned signal is no longer a time delay but a frequency, since such a resonator acts as a narrowband transducer. Resonators are poorly suited to pulse-mode GPR interrogation since the short sampling duration (typically 5  $\mu\text{s}$  at most) is hardly compatible with an accurate returned signal frequency identification. Indeed, piezoelectric single-crystal substrates exhibit for temperature sensing a maximum sensitivity of 100 ppm, so that the frequency of a 100 MHz transducer must be identified with 10 kHz accuracy



for 1 K accurate temperature measurements. Such an accuracy would require at least a 100- $\mu$ s long record based on basic Fourier transform, or a 20-fold in the frequency identification improvement of the 5- $\mu$ s long record if some assumption (single returned frequency) is made [33]. Furthermore, we have observed that the time reference of pulse-mode GPR hardly provides the needed accuracy for such a precise frequency measurement, and a differential (two resonance frequency identification) approach is mandatory to get rid of delay line ageing and drift, as well as sensor ageing and electromagnetic environmental variations (impedance pulling of the frequency). On the other hand, dedicated interrogation hardware has been developed for probing such narrowband sensors with excellent resolution [34], which happens to work following principles similar to FMCW GPR [35,36]. Actually, FMCW has been demonstrated as an excellent strategy for probing resonators acting as temperature sensors [34].

We demonstrate [8] that assuming the interrogation range of a GPR under given conditions is known – based on radargrams recorded at interfaces with reflection coefficient

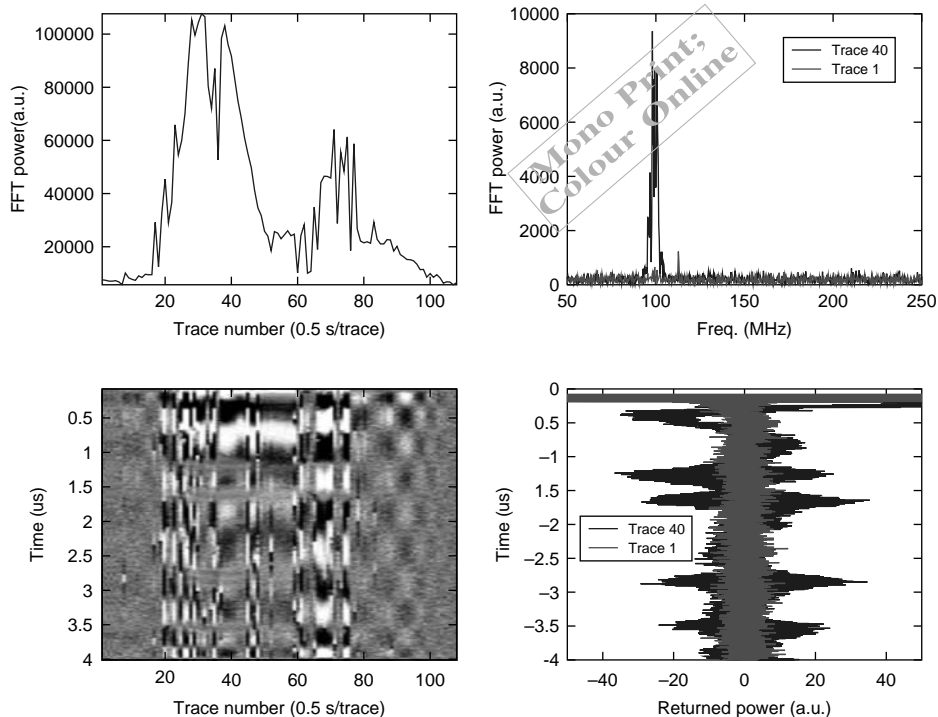


Figure 3. Processing steps for identifying the sensor signal: bottom left, the raw radargram acquired using a 100-MHz antenna set, two-way trip over a 100-MHz delay line acting as a sensor. An 11th-order polynomial fit was removed from each trace to reduce low-frequency background fluctuations from one trace to another. Top right: magnitude of the Fourier transform of the recorded signal, excluding the emitted pulse, exhibiting the returned signal at 100 MHz when the sensor is visible (blue, trace 40) and invisible (red, trace 1). While the magnitude of the Fourier transform is the most visual indicator of the sensor detection, the phase of the Fourier transform at the maximum returned power frequency is the most accurate signature for quantitative information retrieval. Bottom right: comparison of the time domain reflected signal when the sensor is visible (blue, trace 40) and absent (red, trace 1). Top left: the integral of the magnitude of the Fourier transform of the returned power in the 95–105 MHz band is an indicator of the presence of the sensor (the RADAR is located over the sensor at traces 30 and 55).

246  $\Pi_{\text{ice-rock}}$  (e.g. ice–rock interface in our case) – and considering the insertion loss  $\Pi_{\text{SAW}}$  of  
 247 a SAW sensor is known, then the distance  $d_{\text{SAW}}$  at which a sensor can be interrogated is  
 248 given by

$$249 \quad d_{\text{SAW}} = d_{\text{ice-rock}} \times 10^{(\Pi_{\text{ice-rock}} - \Pi_{\text{SAW}})/40}.$$

251 Using typical constants of a reflection coefficient at the ice–rock interface of  $-19$  dB  
 252 (assuming a relative permittivity of ice of 3.1 and 5 for rock) and insertion losses of  
 253  $-35$  dB for an SAW delay line, then the interrogation range of a sensor is 0.4 times that  
 254 found for the ice–rock interface. Considering we are able to gather a usable signal for ice–  
 255 rock interfaces deeper than 100 m, the SAW sensor should be readable at a depth of at least  
 256 40 m. Experimental data were gathered with a sensor buried 5 m deep in snow, exhibiting a  
 257 signal-to-noise ratio consistent with a 40 m maximum depth interrogation range [8].  
 258 Acoustic sensor data analysis when probed by GPR only requires software signal  
 259 processing, and no hardware modification:

- 261 (1) a Fourier transform on the returned signal radargram (Figure 3, bottom left)  
 262 identifies whether a sensor is located within the RADAR interrogation range  
 263 (Figure 3, top right),
- 264 (2) for each trace (Figure 3, bottom right) in which a frequency signature of the sensor  
 265 is identified (Figure 3, top left), the phase of the Fourier component including most  
 266 of the power is indicative of the acoustic delay, and hence of the physical quantity  
 267 under investigation.

#### 268 4. Probing resonators with GPR

269 Pulse-mode GPR is intrinsically wideband devices hardly compliant with most  
 270 radiofrequency regulations, but acceptable for geophysical applications. The antenna  
 271 size – and hence central frequency of the emitted pulse – is usually selected as a trade-off  
 272 between depth resolution (the higher the frequency, the better the resolution) and  
 273 penetration distance of the electromagnetic wave (the lower the frequency, the deeper the  
 274 reflected signal which can be detected). Hence, an associated sensor must adapt to the  
 275 available frequency range of common GPR – typically in the range of 50–1500 MHz.  
 276 Although acoustic delay lines are wideband devices, a given sensor will nevertheless only  
 277 be compatible with a single antenna (100, 200, 400 MHz or above range).

278 SAW delay *lines* are 500  $\mu\text{m}$  thick, 1  $\text{cm}^2$  large sensors: the associated antenna must be  
 279 much larger to be efficient at the incoming electromagnetic wavelength. Although  
 280 the dipole length is reduced thanks to the high relative permittivity of the medium in which  
 281 the sensor is buried, the antenna dimension nevertheless remains in the tens of *centimetres*  
 282 length. A linear polarisation of the antenna connected to the sensor – as provided by the  
 283 most simple geometry of the dipole antenna – also means that the ground-based  
 284 interrogation GPR must be oriented accordingly so that the buried and surface dipoles are  
 285 parallel. We have experimentally observed that in a crossed-polarisation configuration, the  
 286 returned power is too low to allow for a useful measurement, meaning that multiple  
 287 sensors can be located in common view of the GPR and selected through surface antenna  
 288 orientation during the measurement.

#### 291 5. Sensor signal identification

292 Using the same instrument to probe both the buried dielectric and conductivity interfaces  
 293 and sensor signal yields the issue of classifying which reflection is associated with which  
 294

phenomenon. In case of the pulse-mode GPR, two criteria allow for the identification of a sensor signal (Figure 4):

- (1) the design of SAW delay line typically locates the first reflection at least  $1 \mu\text{s}$  after the incoming electromagnetic pulse reaches the sensor. Such a delay (500 ns two-way trip) would be associated with an interface located 42 m deep in ice or 7.5 m deep in water. The signal-to-noise ratio of the reflected signal, associated with a sensor shallower than expected from an electromagnetic propagation, will obviously allow the association of the returned signal with the sensor rather than with a buried interface. Such a classification step is similar to the time-domain multiplexing familiar to radiofrequency communications,
- (2) during the migration post-processing step, the hyperbola curvature on which all points associated with a single point-like reflector lie is dependent on the reflector depth. Since the time delay due to a SAW delay line is associated with an acoustic velocity rather than with the electromagnetic velocity, the curvature of the hyperbola on which the sensor-related echoes lie will be that of a shallow reflector and the automated migration algorithm will not be able to focus all the data on a single point-like reflector.

In the case of narrowband reflectors, the quality factor of acoustic sensors – typically in the 10,000 range below 400 MHz – is much larger than any natural reflector, even dielectric media located between parallel conducting plates acting as reflectors. Hence, the long (several microseconds) time-domain echo, or in the frequency domain the narrowband frequency definition of the returned signal, is hardly missed for a dielectric reflector.

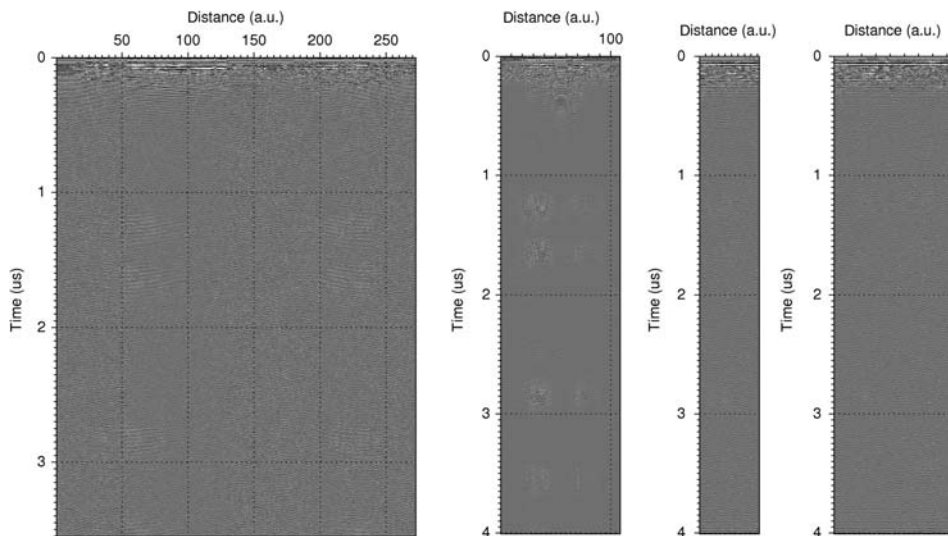


Figure 4. Left to right: two examples of 100-MHz delay line probed with a Malå RAMAC bistatic GPR connected to a 100-MHz dipole antenna (1261 MHz sampling frequency, 4487 and 5060 samples, respectively); two examples of probing a 200-MHz delay line using a Malå RAMAC bistatic GPR connected two 200 MHz dipole antenna (1261 MHz sampling frequency, 5060 samples). The reflections from the sensor are located at delays 1.3, 1.6, 2.8 and  $3.5 \mu\text{s}$ . The first, second and fourth images depict two-way trips over the sensor, while the third image was acquired with only a one-way trip over the sensor. All data processed with the Seismic Unix software.

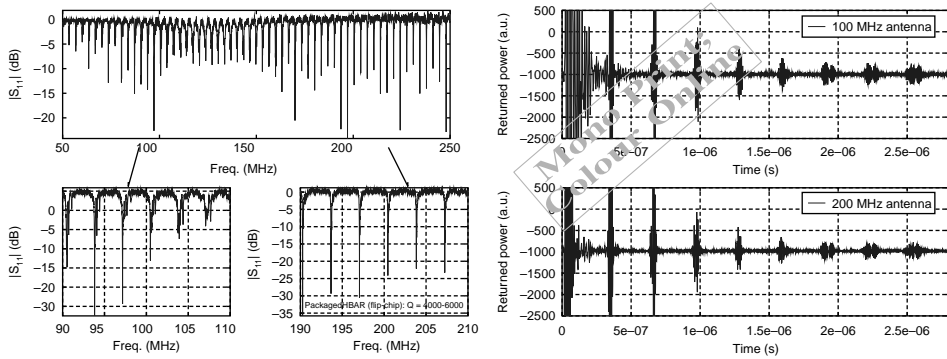


Figure 5. Left: frequency-domain characterisation of an HBAR using a radiofrequency network analyser (Rohde & Schwartz ZVL). Modes are separated by 3-MHz gaps (top: wideband characterisation exhibiting the mode continuum from below 100 MHz to above 200 MHz; bottom left: zoom around the 100 MHz area; bottom right: zoom around the 200 MHz area). Right: time domain characterisation of this same HBAR, with reflections appearing every 300 ns, performed using Malå RAMAC 100 MHz antenna (top) and 200-MHz antenna (bottom). Since the acoustic velocity of the wave changes with physical properties of the environment of the HBAR, the time delay between successive reflections is an indicator of such physical properties. This particular HBAR design exhibits little temperature coefficient of frequency, and hence little velocity dependence with temperature, providing useful tagging information.

## 6. Novel resonator design for use with GPR

In order to provide a sensor configuration compatible with multiple antenna geometries, e.g. compatible with the frequency range of 100–400 MHz, a frequency comb must be generated over this frequency range. One geometry which appears promising for such a purpose is the HBAR [37] configuration in which a bulk acoustic wave is confined inside a low-acoustic loss thick (300–500  $\mu\text{m}$ ) substrate, while the high-operating frequency condition is defined by a thin (< 100  $\mu\text{m}$ ) piezoelectric layer coated on the dielectric substrate. The broadband envelope of the transfer function (Figure 5, left) – here with a maximum returned power around 200 MHz – is defined by the piezoelectric layer thickness, and the comb period (whether in time or frequency domain) by the thickness of the thick substrate. We have demonstrated high-quality factor and wide frequency operation range with such a configuration (Figure 5, right): the 1  $\times$  1 mm HBAR is connected to 2  $\times$  40 cm enamelled wire dipole antenna.

## 7. Conclusion

Beyond the use of RADARs in general and GPR in particular for probing passive reflectors, we demonstrate that acoustic wave devices are perfectly suited as cooperative targets for monitoring physical quantities thanks to existing RADAR systems. Both wideband sensors – acoustic delay lines – and narrowband sensors – resonators – are suited for the various classical RADAR measurement strategies, namely pulse-mode and FMCW measurements. The recorded signals require no modification of the hardware, and identifying the physical quantity under investigation only requires post-processing of the data to extract either an accurate time delay (as a phase between successive echoes in the wideband strategy) or frequency (in the FMCW narrowband strategy), both of which are representative of the acoustic velocity in the sensor and hence the physical quantity affecting most significantly the sensor behaviour thanks to a design reducing the influence of unwanted velocity variation

sources. Furthermore, a differential approach in which sensors with different behaviours to external disturbances are interrogated reduces the influence of correlated noise, ageing and local time reference drift.

### Acknowledgements

Part of the funding for this project was provided by the French National Research Agency (ANR) under the Cryo-Sensors grant.

### References

- [1] G. Clemena, *Handbook on Nondestructive Testing of Concrete*, 2nd ed., CRC Press 2003.
- [2] T. Saarenketo and T. Scullion, *Road evaluation with ground penetrating radar*, *J. Appl. Geophys.* 43 (2000), pp. 119–138.
- [3] National Research Council Rexford M. Morey, *Ground Penetrating Radar for Evaluating Subsurface Conditions for Transportation Facilities*, American Association of State Highway and Transportation Officials, National Cooperative Highway Research Program, National Academy Press, Washington, DC, 1998.
- [4] K. Maser, *Condition assessment of transportation infrastructure using ground-penetrating radar*, *J. Infrastruct. Syst.* 2 (1996), pp. 94–101.
- [5] G. Brooker, *Sensors and Signals*, Australian Centre for Field Robotics 2007.
- [6] B. Lipták, *Level Measurement*, Vol. 1, Chapter 3, CRC Press 2003.
- [7] C. Allen, K. Shi, and R. Plumb, *The use of ground-penetrating radar with a cooperative target*, *IEEE Trans. Geosci. Remote Sensing* (1998), pp. 1821–1825.
- [8] J.M. Friedt, T. Rétoznaz, S. Alzuaga, T. Baron, G. Martin, T. Laroche, S. Ballandras, M. Griselin, and J.P. Simonnet, *Surface acoustic wave devices as passive buried sensors*, *J. Appl. Phys.* 109 (2011), p. 034905.
- [9] R. White and F. Voltmer, *Direct piezoelectric coupling to surface acoustic waves*, *Appl. Phys. Lett.* 7 (1965), pp. 314–316.
- [10] X.Q. Bao, W. Burkhard, V.V. Varadhan, and V. Varadan, *SAW temperature sensor and remote reading system*, *IEEE Ultrasonics Symposium*, 1987, pp. 583–585.
- [11] W. Buff, S. Klett, M. Rusko, J. Ehrenpfordt, and M. Goroli, *Passive remote sensing for temperature and pressure using SAW resonator devices*, *IEEE Trans. Ultrason. Ferroelectrics Freq. Contr.* 45 (1998), pp. 1388–1392.
- [12] G. Scholl, F. Schmidt, T. Ostertag, L. Reindl, H. Scherr, and U. Wolff, *Wireless passive SAW sensor systems for industrial and domestic applications*, *IEEE International Frequency Control Symposium*, Pasadena, CA, 1998, pp. 595–601.
- [13] W. Bulst, G. Fischerauer, and L. Reindl, *State of the art in wireless sensing with surface acoustic waves*, *IEEE Trans. Indus. Electronics* 48 (2001), pp. 265–271.
- [14] L. Reindl and I. Shrena, *Wireless measurement of temperature using surface acoustic waves sensors*, *IEEE Trans. Ultrason. Ferroelectrics Freq. Contr.* 51 (2004), pp. 1457–1463.
- [15] S. Schuster, S. Scheibelhofer, L. Reindl, and A. Stelzer, *Performance evaluation of algorithms for SAW-based temperature measurement*, *IEEE Trans. Ultrason. Ferroelectrics Freq. Contr.* 53 (2006), pp. 1177–1185.
- [16] A. Pohl, R. Steindl, and L. Reindl, *The ‘intelligent tire’ utilizing passive SAW sensors – measurement of tire friction*, *IEEE Trans. Instrum. Meas.* 48 (1999), pp. 1041–1046.
- [17] J. Beckley, V. Kalinin, M. Lee, and K. Voliansky, *Non-contact torque sensor based on SAW resonators*, *IEEE International Frequency Control Symposium and PDA Exhibition*, 2002, pp. 202–213.
- [18] H. Scherr, G. Scholl, F. Seifert, and R. Weigel, *Quartz pressure sensor based on SAW reflective delay line*, *IEEE Ultrasonics Symposium*, 1996, pp. 347–350.
- [19] G. Bruckner, A. Stelzer, L. Maurer, J. Biniash, L. Reindl, R. Teichmann, and R. Hauser, *A high-temperature stable SAW identification tag for a pressure sensor and a low-cost interrogation unit*, *IEEE Sensor*, 2003, pp. 467–472.
- [20] H. Oh, W. Wang, K. Lee, I. Park, and S. Yang, *Sensitivity improvement of wireless pressure sensor by incorporating a SAW reflective delay line*, *Int. J. Smart Sens. Intell. Syst.* 1 (2008), pp. 940–954.

- 442 [21] Y. Dong, W. Cheng, S. Wang, Y. Li, and G. Feng, *A multi-resolution passive SAW chemical*  
 443 *sensor*, *Sensors Actuators B* 76 (2001), pp. 130–133.
- 444 [22] W. Seidel and T. Hesjedal, *Multi-frequency and multi-mode GHz surface acoustic wave sensor*,  
 445 *IEEE Ultrasonics symposium*, 2003, pp. 1408–1411.
- 446 [23] M. Dierkes and U. Hilleringmann, *Telemetric surface acoustic wave sensor for humidity*, *Adv.*  
 447 *Radio Sci.* 1 (2003), pp. 131–133.
- 448 [24] A. Pohl, F. Seifert, L. Reindl, G. Scholl, T. Ostertag, and W. Pietsch, *Radio signals for SAW ID*  
 449 *tags and sensors in strong electromagnetic interference*, *IEEE Ultrasonics Symposium*, 1994,  
 450 pp. 195–198.
- 451 [25] L. Reindl, G. Scholl, T. Ostertag, W. Ruile, H. Scherz, R. Ruppel, and F. Schmidt, *Wireless*  
 452 *remote identification and sensing with saw devices*, *Sensor*, 1997, pp. 161–166.
- 453 [26] C. Hartmann, *A global SAW ID tag with large data capacity*, *Proceedings of 2002 IEEE*  
 454 *Ultrasonics Symposium*, 2002, pp. 65–69.
- 455 [27] J. Han, R. Xu, and C. Nguyen, *On the development of a low-cost, compact planar integrated-*  
 456 *circuit sampling receiver for UWB systems*, *Ultra-Wideband, Short-Pulse Electromagnetics*,  
 457 Vol. 8, Springer 2007, pp. 161–170.
- 458 [28] H.P. Marshall and G. Koh, *FMCW radars for snow research*, *Cold Reg. Sci. Technol.* 52  
 459 (2008), pp. 118–131.
- 460 [29] V. Plessky and L. Reindl, *Review on SAW RFID tags*, *IEEE Trans. Ultrason. Ferroelectrics*  
 461 *Freq. Contr.* 57 (2010), pp. 654–668.
- 462 [30] J. Kuypers, L. Reindl, S. Tanaka, and M. Esashi, *Maximum accuracy evaluation scheme for*  
 463 *wireless saw delay-line sensors*, *IEEE Trans. Ultrason. Ferroelectrics Freq. Contr.* 55 (2008),  
 464 pp. 1640–1652.
- 465 [31] S. Kim, S. Carnes, A. Haldemann, E. Ng, and S. Arcone, *Miniature ground penetrating radar*,  
 466 *CRUX GPR*, *IEEE Aerospace Conference*, 2006.
- 467 [32] J. Davis and A. Annan, *Ground penetrating radar for high resolution mapping of soil and rock*  
 468 *stratigraphy*, *Geophys. Prospect.* 37 (1989), pp. 531–551.
- 469 [33] D. Rife and R. Boorstyn, *Single-tone parameter estimation from discrete-time observations*,  
 470 *IEEE Trans. Inform. Theory* IT-20 (1974), pp. 591–598.
- 471 [34] G. Hofbauer, *FMCW based readout system accuracy enhancement techniques for surface*  
 472 *acoustic wave RFID sensors*, *IEEE/MTT-S International Microwave Symposium*, 2007,  
 473 pp. 575–578.
- 474 [35] S. Scheiblhofer, S. Schuster, M. Jahn, R. Feger, and A. Stelzer, *Performance analysis of*  
 475 *cooperative FMCW radar distance measurement systems*, *IEEE MTT-S International*  
 476 *Microwave Symposium Digest*, 2008, pp. 121–124.
- 477 [36] J.M. Friedt, C. Droit, G. Martin, and S. Ballandras, *A wireless interrogation system exploiting*  
 478 *narrowband acoustic resonator for remote physical quantity measurement*, *Rev. Sci. Instrum.*  
 479 81 (2010), p. 014701.
- 480 [37] D. Gachon, E. Courjon, G. Martin, L. Gauthier-Manuel, J.C. Jeannot, W. Daniau, and S.  
 481 *Ballandras*, *Fabrication of high frequency bulk acoustic wave resonator using thinned single-*  
 482 *crystal lithium niobate layers*, *Ferroelectrics* 362 (2010), pp. 30–40.
- 483  
484  
485  
486  
487  
488  
489  
490